Sol–gel synthesis, properties and protein loading/ delivery capacity of hollow bioactive glass nanospheres with large hollow cavity and mesoporous shell

Ahmed EL-FIQI (✉)

Glass Research Department, National Research Centre, Cairo 12622, Egypt

E-mail: dr.ahmed.elfiqi@gmail.com

Supplementary materials

To further explore and understand the *in vitro* release kinetics and release mechanism of Cyto *c*, the experimental Cyto *c* release data were fitted to different kinetic models (Fig. S1 and Table S1) including zero-order (Eq. (S1)), first-order (Eq. (S2)), Higuchi (Eq. (S3)), Hixson–Crowell (Eq. (S4)) and Korsmeyer–Peppas (Eq. (S5)) [S1]:

$$Q_t = Q_o + k_0 t \tag{S1}$$

$$\lg Q_t = \lg Q_o - \frac{k_1 t}{2.303} \tag{S2}$$

$$Q_t = k_H t^{1/2} \tag{S3}$$

$$Q_o^{1/3} - Q_t^{1/3} = k_{HC} t \tag{S4}$$

$$\lg Q = n \lg t + \lg k \tag{S5}$$

where, Q_t is the amount of drug released over time t, Q_o is the initial amount of drug in solution, k_0 and k_1 are the zero- and the first-order release rate constants, k_H is the Higuchi dissolution constant, k_{HC} is the Hixson–Crowell constant, k is a rat constant, and n is an exponent related to the release mechanism. To compare these models, the coefficient of determination (R^2) was obtained by fitting experimental release data to linearity. Here, the coefficient of determination, R^2, represents the goodness of the fit to the experimental data. The higher the R^2 value (the closer to 1), the better the model fits the data. The results of the fitted kinetic models are shown in Table S1. As can be concluded, the Korsmeyer–Peppas model has the highest R^2 value (R^2 = 0.9653) followed by Higuchi (R^2 = 0.8984). However, fitting the release of Cyto *c* to zero-order (describes the systems where the release rate is concentration independent), first-order (describes the systems where release rate is concentration dependent), and Hixson–Crowell (describes the release from systems where there is a change in surface area and diameter of particles) kinetic models gave rise to lower R^2 values (Table S1) and thus the release kinetics and release mechanism of Cyto *c* from HBGn cannot be described by these kinetic models. The Korsmeyer–Peppas model describes the release kinetics and release mechanism from swellable as well as non-swellable systems. Whereas, the Higuchi model describes the release kinetics from insoluble systems as a square root time-dependent process based on the Fick's diffusion law. Accordingly, a time-dependent and diffusion-controlled Cyto *c* release from HBGn followed the Fick's diffusion law. The values of release rate constant k and the release exponent n are listed in Table S1. The value of the release exponent n indicates the mechanism of release, where a value of $0 < n \leq 0.45$ suggests diffusion controlled release (Fickian diffusion or quasi-Fickian diffusion) for non-swellable systems [S3], while a value of $0.45 < n < 0.89$ suggests anomalous diffusion or non-Fickian diffusion (combination of diffusion and erosion) for swellable systems [S4–S5]. As the value of n = 0.33, this is suggesting that the *in vitro* Cyto *c* release is likely to be controlled by a diffusion-controlled process and it can be described by a Fickian diffusion release mechanism.

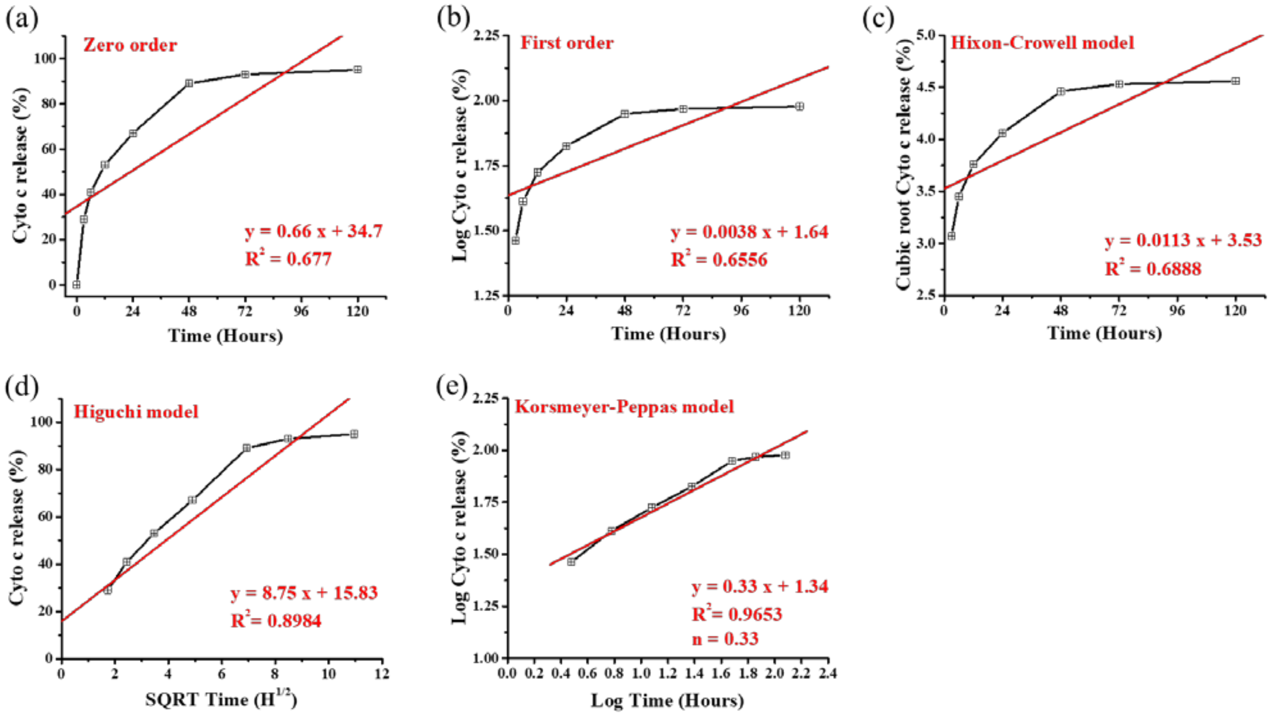

Fig. S1 Fitting of *in vitro* Cyto *c* release to different kinetic models including **(a)** zero-order model, **(b)** first-order model, **(c)** Hixon–Crowell model, **(d)** Higuchi model, and **(e)** Korsmeyer–Peppas model.

Table S1 Summarized kinetic models, kinetic parameters and the corresponding coefficients of determination (R^2) used in the analysis of Cyto *c* release kinetics and its release mechanism

Kinetic model	Kinetic parameters	R^2
Zero-order	Q_o = 34.7%, k_0 = 0.66 h^{-1}	0.6772
First-order	Q_o = 1.64%, k_1 = 0.0038 h^{-1}	0.6556
Hixon–Crowell	Q_o = 13.53%, k_{HC} = 0.0113 h^{-1}	0.6888
Higuchi	k_H = 8.75% $h^{-1/2}$	0.8984
Korsmeyer–Peppas	n = 0.33, k = 1.34 $h^{-0.33}$	0.9653

References

[S1] Shariatinia Z, Pourzadi N. Designing novel anticancer drug release vehicles based on mesoporous functionalized MCM-41 nanoparticles. Journal of Molecular Structure, 2021, 1242: 130754

[S2] Lotfalian S, Nematollahzadeh A, Ghasemi S. Hierarchically structured protein-based hollow-nanospheres for drug delivery. Reactive and Functional Polymers, 2021, 160: 104821

[S3] Joy M, Iyengar S J, Chakraborty J, et al. Layered double hydroxide using hydrothermal treatment: morphology evolution, intercalation and release kinetics of diclofenac sodium. Frontiers of Materials Science, 2017, 11(4): 395–408

[S4] Zhou H-Y, Cao P-P, Zhao J, et al. Release behavior and kinetic evaluation of berberine hydrochloride from ethyl cellulose/chitosan microspheres. Frontiers of Materials Science, 2014, 8(4): 373–382

[S5] Ge M, Li Y, Zhu C, et al. Preparation of organic-modified magadiite–magnetic nanocomposite particles as an effective nanohybrid drug carrier material for cancer treatment and its properties of sustained release mechanism by Korsmeyer–Peppas kinetic model. Journal of Materials Science, 2021, 56(25): 14270–14286